Solvothermal synthesis of ultra-fine silver nanowires with a diameter about 20 nm and an aspect ratio approximately 2000 for highly conductive flexible transparent film

Yuxiu Li[1] · Ximin Yuan[1] · Hongwei Yang[1] · Yunxiu Chao[1] · Shuailong Guo[1] · Chuan Wang[1]

Abstract

Flexible transparent conductive films (TCFs) based on silver nanowires (AgNWs) networks have been widely researched as an alternative to indium tin oxide (ITO) for optoelectronic devices. However, AgNW-based TCFs still involve issues such as high haze and poor transmittance for practical application. The innovation point of our work is the synthesis of ultra-fine and high aspect ratio AgNWs, and they are developed to prepare high-performance AgNW-based TCFs. In this study, a rapid and rationally designed method to synthesize ultra-fine AgNWs through dual ionic assistants assisted has been explored. As a result, the as-synthesized AgNWs have a uniform ~ 20 nm diameter, and a high aspect ratio of 2000, which are the minimum diameter and maximum aspect ratio among the values reported previously for solvothermal-processed AgNWs. A highly transparent and bendable AgNW-based conductive film shows a 97.71% transmittance and a haze of 1.49% under the condition of disregarding the transmittance and haze of bare PET substrate. The sheet resistance (R_{sheet}) of the resulting AgNW-based conductive film is ~ 15 Ω sq^{-1}. Most importantly, the AgNW-based conductive film exhibits strong adhesion to the substrate. The advanced and wide-ranging features of the as-prepared AgNW-based conductive film greatly contribute to its use as a transparent conductive film in multifunctional flexible optoelectronic devices.

1 Relevance summary

In this paper, ultra-fine silver nanowires with a diameter about 20 nm and an aspect ratio approximately 2000 were prepared by a simple solvothermal process. To the best of our knowledge, the synthesis of AgNWs with diameters < 40 nm is still difficult, and there is no report use solvothermal and not attach any external pressure to control the growth of AgNWs to obtain AgNWs with a small diameter. This research uses hydroxyethyl cellulose as a crucial film-forming adhesive, which has a characteristic of green environmental protection. The AgNW-based conductive film offers an excellent photoelectric property, which presents more obvious advantages compared with previous reports.

✉ Hongwei Yang
nanolab@ipm.com.cn

1   State Key Laboratory of Advanced Technologies
     for Comprehensive Utilization of Platinum Metals,
     Kunming Institute of Precious Metals, Kunming 650106,
     People's Republic of China

2 Introduction

Transparent conductive films (TCFs) play a pivotal role in a variety of optoelectronic devices, including touch panels [1], liquid crystal displays [2], transparent organic light-emitting diodes (OLEDs) [3], thin-film solar cells [4], and conducting film glasses [5], due to its high electric conductivity and high transmissivity within the range of visible light. With the transformation and upgrading of consumer electronics industry, and the rapid development of display technology, an industrial demand for flexible, pliable, and even stretchable TCFs to replace the expensive, rigid, and brittle indium tin oxide (ITO) thin films. Until now, emerging candidates have been proposed as replacements for ITO, including silver nanowires (AgNWs) [6–8], metal grids [9, 10], graphene [11, 12], conductive polymers [13], carbon nanotubes [14], and ITO ink [15]. Among these alternatives, AgNWs can provide good electrical conductivity, remarkable optical transparency, excellent mechanical flexibility, and compatibility with inexpensive processing. These superiorities make AgNWs become most promising potential alternative as a next generation TCFs. Significantly, it has been

theoretically predicted and experimentally proved that thin and long AgNWs are beneficial to the performance of the TCFs, especially for high-level applications such as pony-size touch panel screens that require low haze and low resistance under extremely high transparency conditions [16]. Therefore, it is extremely critical to employ AgNWs with a small diameter and a large aspect ratio to prepare TCFs.

Over the past few years, the polyol reduction process has been the most universal synthetic method for preparing AgNWs [17–19]. Although the method as the most common method has substantial advantages, there are also some obvious disadvantages, limiting its practical application. Specifically, in the polyol reduction process, various influence factors such as stirring speed, injection speed of chemicals, and number of injection have almost always affected the morphology of AgNWs, including length, diameter, and surface structure, resulting in an tough experimental condition and intricate synthesis process. Moreover, and in general, AgNWs synthesized by the polyol reduction route have an average diameter larger than 40 nm and an aspect ratio < 1000. In contrast, the solvothermal process is more convenient and easier, and can achieve one-step synthesis. Most recently, synthesis of AgNWs by solvothermal method has been reported. However, to the best of our knowledge, the synthesis of AgNWs with diameters < 40 nm is still difficult, and there is no report on the utilization of solvothermal with dual ionic assistants, and not attach any external pressure to control the growth of AgNWs to obtain AgNWs with a small diameter and a large aspect ratio, which are summarized in Table 1 [20–24]. Chen et al. [20] demonstrated that the AgNWs were successfully synthesized by solvothermal process, but unfortunately their diameter ranging from 56.6 to 84.2 nm and aspect ratio ranging from 100 to 500, and far below actual requirements. Fang et al. [21] claimed that the as-synthesized AgNWs have a typical wire like structure; however, the length is below 31.2 µm with diameter over 910 nm, and the aspect ratio reached only around 35. Liu et al. [22] experimentally showed that AgNWs were synthesized via a solvothermal method, with diameter ranging from 50 to 100 nm and 5–10 µm in length. Banica et al. [23] also independently showed that AgNWs diameter between 200 and 250 nm and length between 10 and 25 µm, can be obtained by controlling the solvent composition. Therefore we can conclude that it is urgent to achieve the synthesis of thin and long AgNWs.

Herein, AgNWs with an average diameter of ~ 20 nm and an average length of ~ 40 µm have been first synthesized via a solvothermal method with dual ionic assistants, and not attach any external pressure. Meanwhile, we demonstrate the film of AgNWs network on a polyethylene glycol terephthalate (PET) substrate via bar coating. The AgNW-based conductive film offers a sheet resistance (R_{sheet}) of ~ 15 Ω sq^{-1} with a 97.71% transmittance and a haze of 1.49%. And most importantly, the AgNW-based conductive film exhibits strong adhesion to the substrate.

3 Experimental

3.1 Chemicals and materials

Silver nitrate (AgNO$_3$, ≥ 99.8%, STREM), poly-vinylpyrrolidone (PVP, Mw ~ 1,300,000, Aldrich), sodium chloride (NaCl, ≥ 99.5%, Sinopharm), potassium bromide (KBr, ≥ 99.0%, Sinopharm), ethylene glycol (EG, ≥ 99.0%), hydroxyethyl cellulose (HEC, Dow-QP-100MH), ethanol (C$_2$H$_5$OH, ≥ 99.0%) and PET were purchased from commercial sources. All the reagents were analytical grade reagents and used as received without any further purification. Deionized (DI) water was prepared by laboratory water purification system with a resistivity of not < 18.2 MΩ cm and an operating temperature of 20 °C, and it was used throughout the experiment.

3.2 Preparation of AgNWs

Ultra-fine silver nanowires were obtained through a dual ionic assistants assisted synthesis process. Typically, 100 mL of ethylene glycol solution of NaCl with a concentration of 0.0086 mol L^{-1}, and 100 mL of ethylene glycol solution of KBr with a concentration of 0.0042 mol L^{-1} were firstly prepared. Subsequently, transfer 5 mL of NaCl solution and 5 mL of KBr solution to 90 mL of ethylene glycol. Meanwhile, 1.12 g of AgNO$_3$ and 6.95 g of PVP were dissolved into 150 mL of ethylene glycol, to form homogeneous

Table 1 Comparison of AgNWs synthesized by solvothermal method

Method	Diameter (nm)	Length (µm)	Aspect ratio	References
Solvothermal method	56.6–84.2	8.63–29.8	100–550	[20]
	910	31.2	~35	[21]
	50–100	5–10	50–200	[22]
	80	3	~40	[23]
	97	78	~800	[24]
Solvothermal method	~20	~40	~2000	This work

solution. Later, the former solution was poured into the mixed solution of NaCl and KBr. After magnetically stirring for 10 min, a light white suspension was obtained. 250 mL of the suspension was transferred into a Teflon-lined stainless steel autoclave with a capacity of 500 mL and was reacted under solvothermal condition at 170 °C for 2 h 10 min with a ramping rate of 6 °C min^{-1} at an oven. After reaction finished, the autoclave was taken out and cooled under atmospheric conditions. The free-standing AgNWs was collected by centrifugation of 4800 rpm for about 20 min and washed repeatedly by ethanol and deionized water, respectively. Finally, a black green sample was obtained. The sample was dispersed in a small volume of deionized water, and the suspension liquid was filtered through a sieve (aperture: 400 mesh) to remove the agglomerated AgNWs. After this, the solid content of AgNWs was measured.

3.3 Preparation of AgNW ink

A water-soluble AgNWs conductive ink was prepared using HEC as matrix resin. The matrix resin was used as adhesive. First, 1.0 g HEC was stirred in 100 mL of deionized water for 90 min at 60 °C to obtain a uniformly dispersed liquid. Then, transfer 5 mL of above HEC solution and 15 mL of aqueous AgNWs dispersion solution with the solid content

of 0.67% to beaker. Subsequently, two types of solutions were mixed together to form the final ink.

3.4 Preparation of AgNW-based TCFs

The PET substrate was adsorbed onto the platform of the bar coater (BEVS1811/2) by vacuum. After this, the bar (a diameter of 20 μm) was put down to hold the substrate. The AgNW ink was added to the substrate using a dropper. The coating speed and distance were set as at 300 mm s^{-1} and 15 cm, respectively. Later, the bar pushed the conductive ink to glide over the substrate. The obtained wet film was taken down and put in an oven at 130 °C for curing 5 min, and the resulting AgNW-based flexible transparent conductive film was obtained, the thickness of film containing the bare substrate is ~120 μm. The most suitable curing temperature and time should help the AgNW network obtain the best uniformity. In view of the above experimentation, the synthesis of ultra-fine AgNWs and the preparation of AgNW-based TCFs as illustrated in Fig. 1.

3.5 Characterization

The phase constitution identification of the sample was made by X-ray diffraction (XRD, Rigaku TTRIII) with a Cu K_α ($\lambda = 1.54056$ Å) radiation source. All the measurements were

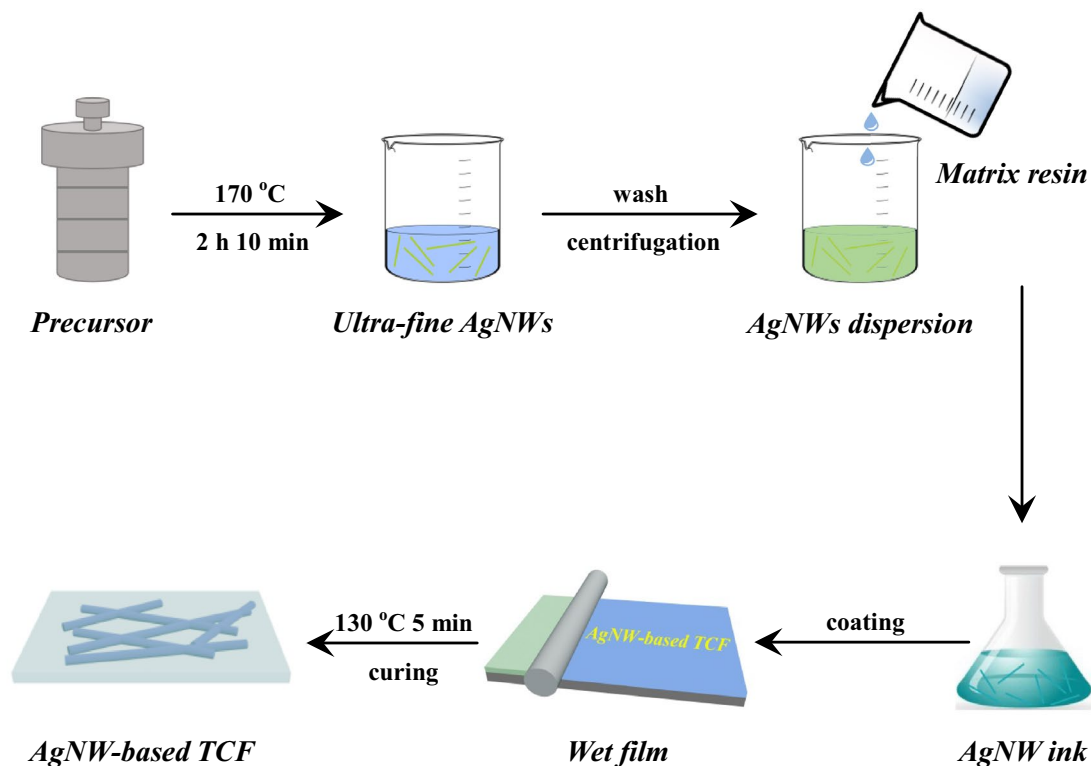**Fig. 1** Typical technology flow diagram of preparation of ultra-fine AgNWs and AgNW-based TCFs

performed in the 2θ range 20°–90° in steps of 0.02° s⁻¹. The microstructures and morphologies of the sample were characterized by field emission scanning electron microscopy (FE-SEM, JSM-7800F, operating at 15 kV). The detailed microstructures of the sample were also determined using transmission electron microscopy (TEM), fast fourier transform (FFT), and high-resolution transmission electron microscopy (HRTEM, JEOL JEM-2100) with an acceleration voltage of 200 kV. The sample was dispersed in ethanol and dropped on copper grids for measurement. The UV–Vis spectra of the sample were recorded by UV–Vis spectrophotometer (PERSEE Genera TU-1901) with a scan range from 190 to 900 nm. The transmittance and haze of the AgNW-based TCFs were obtained using transmittance and haze analyzer (SGW-820), and a bare PET film was used as blank contrast group. The sheet resistance of the AgNW-based TCFs was measured via a four point probe (SB100A/2). The adhesion of the AgNW conductive ink on the PET substrate was performed by tape test. All measurements were performed in air under ambient conditions.

4 Results and discussion

The as-prepared AgNWs were investigated by XRD and the result is displayed in Fig. 2, which is verified as a pure phase by comparing with JCPDS number of 99-0094. As is evident, no other secondary or amorphous phase is found from the XRD pattern. All diffraction peaks can be indexed to the face-centered cubic (fcc) Ag crystal with a space group of *Fm-3 m* (255) and an $a=b=c=4.086$ Å lattice constant. Also, from XRD data one can observe that the intensity ratio
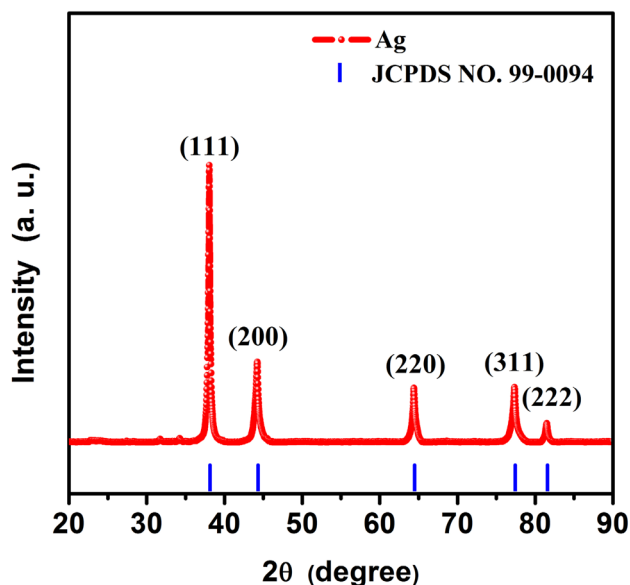

**Fig. 2** Typical XRD pattern of the as-prepared AgNWs

of the reflection (111) exhibits relatively high value, indicating that the grown of AgNWs preferentially along the (111) plane. The average grain size is estimated to be approximately 18 nm using the Scherrer equation ($d=0.943\lambda/\beta\cos\theta$) derived from (111) direction of XRD results. Moreover, the peak sharp and peak intensity suggest that the as-synthesized AgNWs have high crystalline degree.

The morphology and the microstructure of the as-prepared AgNWs are characterized by FE-SEM, as displayed in Fig. 3. The FE-SEM image in Fig. 3a shows a typical wire like structure. The average length of the pristine AgNWs is 40 μm, which is measured based on hundreds of nanowires. It can be observed that the as-prepared AgNWs possesses few silver nanoparticles, indicating the synthetic process will form seed crystal of different shapes. Figure 3b displays the magnified FE-SEM image of as-prepared AgNWs, from which it can be seen that the high purity and uniform AgNWs have been obtained. Moreover, a smooth surface is apparently observed on the magnified FE-SEM image. From high magnification FE-SEM images in Figs. 3c, d, the as-prepared AgNWs with a diameter of ~20 nm are presented in the images. The long AgNWs with thin diameter gives a high aspect ratio of 2000 that is conducive to a high performance AgNW-based film. From the theory of percolation, a certain amount of AgNWs is required for the network to percolate. The thinner and longer the AgNWs, the less number of AgNWs needs to form conductive network, which can increase effectively the transmittance and reduce the haze [25].

The TEM, high resolution TEM and FFT micrographs of as-prepared AgNWs provide more information about the structure characteristics, as shown in Fig. 4. As can be seen from the low magnification TEM images (Fig. 4a, b), the as-prepared AgNWs are thin and uniform in diameter, which have a narrow size distribution. Magnified TEM images have given further insight into the structure, as shown in Fig. 4c, d. Figure 4c shows a smooth surface of the as-prepared AgNWs. Figure 4d displays the tip of an individual AgNW, clearly manifesting the existence of a twin-plane structure parallel to the crystal growth direction, and the pentagonal cross tip demonstrates the formation of a five-fold twinned structure. In order to further confirm the crystalline structure of AgNWs, high resolution TEM image is carried out, as shown in Fig. 4e. It is observed that there is an obvious capping layer with an average thickness of 2.2 nm on the surface of a single AgNW, corresponding to the residual PVP. The PVP layer is difficult to completely eliminate, even after wash and centrifuge repeatedly. On the one hand, PVP plays a vital role in the preparation of AgNWs, as it is used to control effectively the growth of AgNWs and disperse AgNWs by encapsulating encapsulating the {100} planes of AgNWs. On the other hand, contact resistance between AgNWs is caused by residual PVP layer, adsorbing on the

Fig. 3 FE-SEM micrographs of the as-prepared AgNWs at **a** low magnification, **b** relatively high magnification and **c**, **d** high magnification, respectively
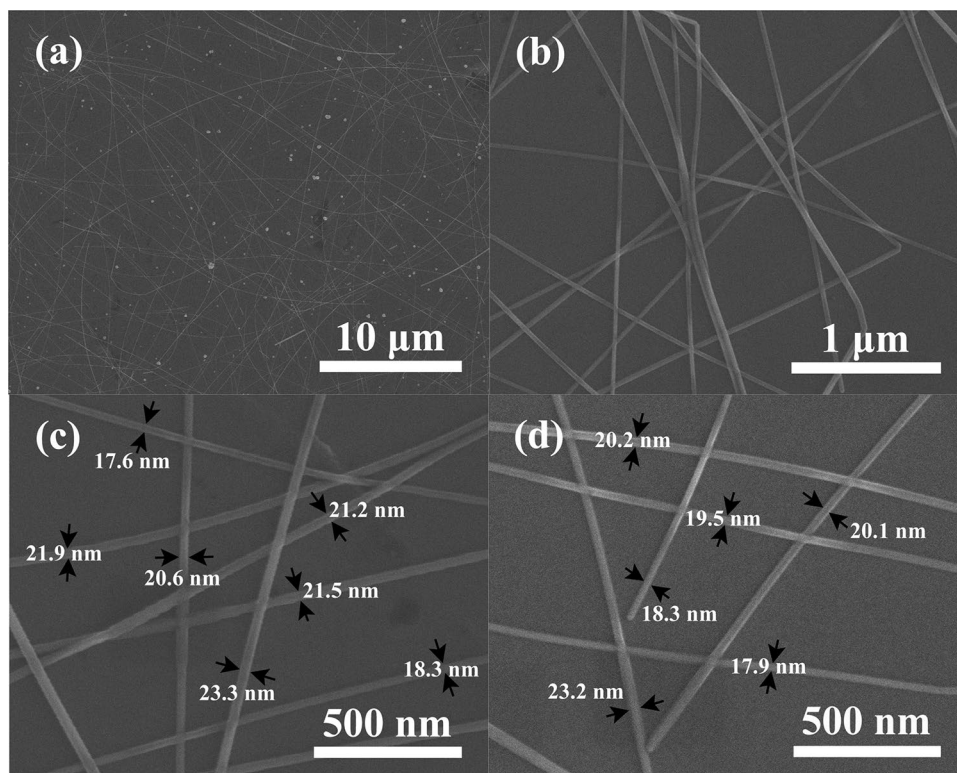
surface of AgNWs and leading to loose contact between AgNWs, which induces capacitive junctions [26]. The diameter of a single AgNW is measured to be about 20 nm, which effectively supports the above SEM measurement. The special part marked by the red line is magnified and shown in inset. The clear well-developed lattice fringes imply a high crystallinity and single orientation. The inset shows lattice fringes with an interplanar spacing of ~ 0.24 nm, which is consistent with (111) plane of faced-centered cubic phase of Ag, and in good agreement with XRD results. It is also reveals that AgNWs are enclosed with the {111} plane acting as the surface plane with a corresponding growth direction of [422], which is consistent with reported values [27]. Furthermore, the FFT pattern (Fig. 4f) further proves that AgNWs possess a twin crystalline structure.

To explain the possible formation mechanism of thin and long AgNWs by dual ionic assistants assisted method, systematic formation process of AgNWs from the nucleation to growth stages has been carried out and shown in Fig. 5. The role of dual ionic assistants, especially the existence of KBr, plays a key part in control of the size of Ag seeds and the diameter of Ag nanowires. Firstly, in the preheating stage, AgCl and AgBr seeds are primarily formed. When the temperature rises to 170 °C, the Ag^+ is continuously reduced to Ag. Meanwhile, a certain amount of multiply twinned particles (MTPs) and nanoparticles are taken shape on the surface of seeds. Then the MTPs grow into silver nanorods and further grow into nanowires under the action of PVP.

During the formation of AgNWs in this work the Br^- can more effectively passivate the {100} planes and limit its growth [28], leading to the synthesis of thinner AgNWs. On the other hand, the AgBr seeds are smaller than the AgCl seeds [29], the smaller AgBr seeds thus promote the formation of ultra-fine AgNWs.

The UV–Vis absorption spectra of as-prepared AgNWs are shown in Fig. 6. It is well known that the UV–Vis spectroscopy can be used to analyze the morphology of AgNWs because the Ag nanostructures have different sizes and shapes exhibit surface plasmon resonance (SPR) bands at different frequencies. In general, there are two plasmon absorption resonances for AgNWs; one is attributed to the transverse oscillation of electrons with the peak around 354 nm, while the second plasmon is due to the oscillation of electrons along the long axis [30]. Figure 6 shows the typical absorption peaks are at 353.43 nm and 369.95 nm, respectively. Meanwhile, no other absorption peaks were obtained by UV–Vis spectroscopy, which further confirm the synthesis of AgNWs. In additional, it has been reported that if the diameter of AgNWs is sufficiently small, it will lead to the blue-shift of absorption peaks, and the large characteristic frequency will < 370 nm [31]. The blue-shift phenomenon is due to a reduction in diameter of the nanostructures, and causes further a reduction of scattered light. This suggests that the as-synthesis AgNWs are ultra-fine AgNWs.

To further analyze and illuminate the characteristics of as-synthesized ultra-fine AgNWs, the appearance features

Fig. 4 **a**, **b** Low magnification TEM micrographs of the as-prepared AgNWs, **c**, **d** high magnification TEM images of the as-prepared AgNWs, **e** the corresponding HRTEM image with obvious lattice fringes, and **f** a corresponding FFT pattern
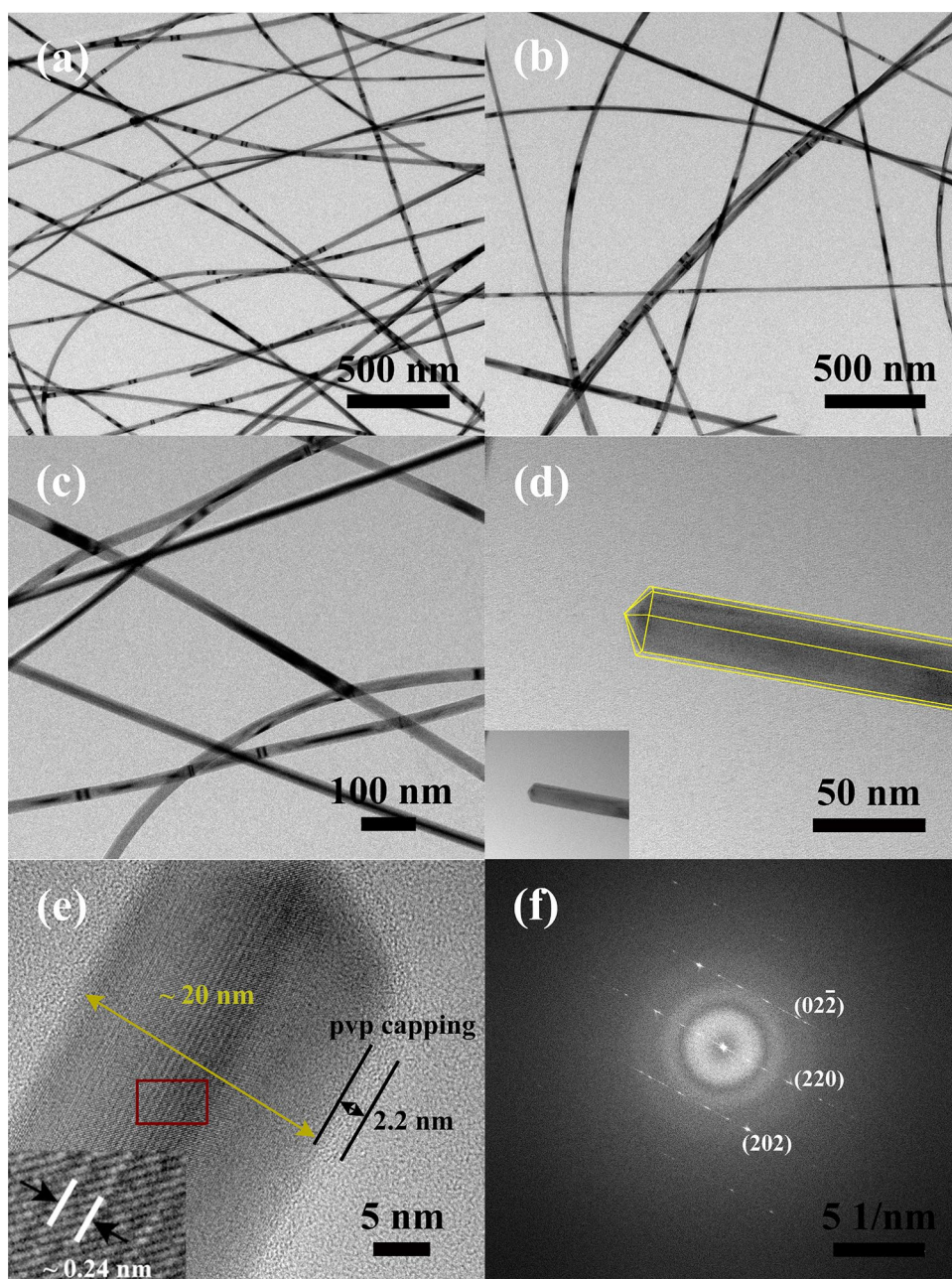
are recorded by optical image, and as displayed in Fig. 7a. As can be seen from the Fig. 7a, the aqueous AgNWs dispersion is the nearest to an atrovirens, it is a typical color of ultra-fine AgNWs. And for all we know, the more thin the AgNWs, the more dark the exterior colour, which further confirm the ultra-fine AgNWs are successfully synthesized by solvothermal method without attach external pressure. The uniform colour indicates that the AgNWs have a good dispersibility in deionized water. Figure 7b shows the flexible nature of the as-fabricated AgNW-based TCFs, exhibiting good flexibility and high optical transmittance.

To verify whether the as-prepared ultra-fine and high aspect ratio AgNWs can serve as TCFs with lower haze,

higher transmittance and lower sheet resistance, the photoelectric properties of AgNW-based TCFs were measured, and shown in Fig. 8. As is well known, the bare PET substrate is not completely transparent. Figure 8a displays the transmittance and haze of are 91.92% and 0.96%, respectively, for the bare PET substrate. When the AgNW ink was coated on the PET substrate using bar coater, the transmittance and haze of AgNW-based TCFs are 89.63% and 2.45%, respectively (as shown in Fig. 8b). Therefore, the AgNW film exhibits a 97.71% transmittance and a haze of 1.49% under the condition of disregarding the transmittance and haze of bare PET substrate. The weak fluctuate illustrates that the as-fabricated AgNW-based TCFs
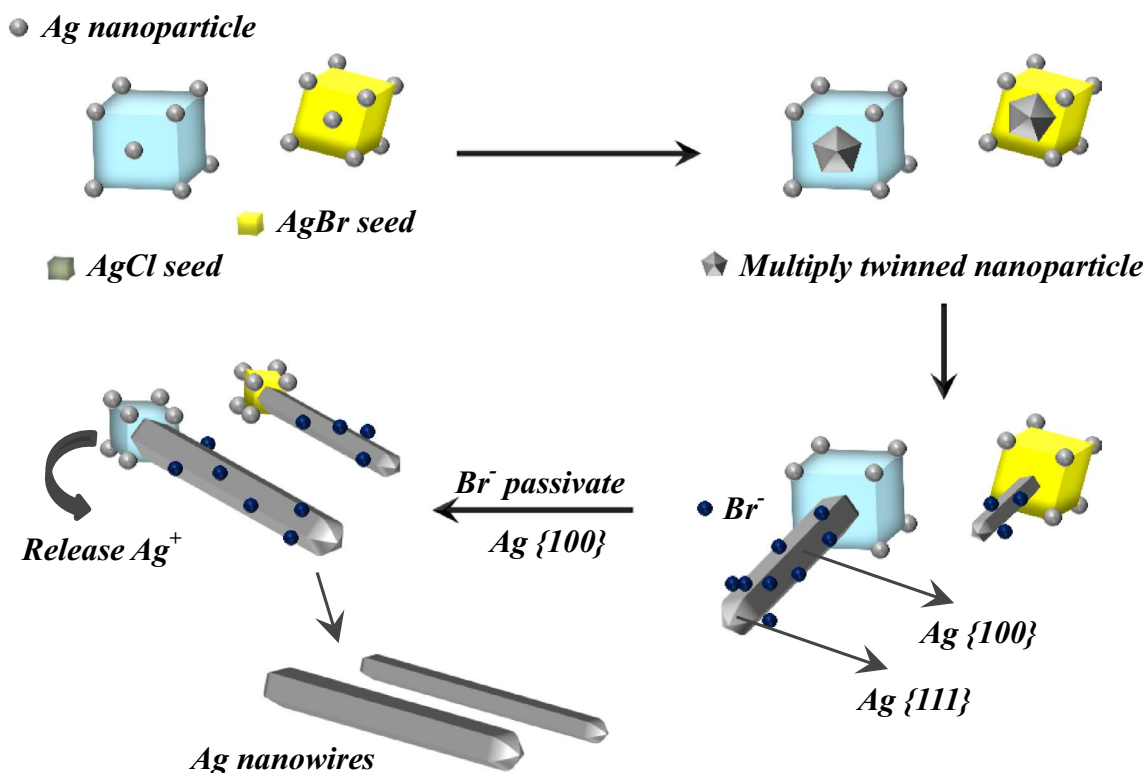
Fig. 5 The possible growth mechanism of ultra-fine AgNWs using dual ionic assistants
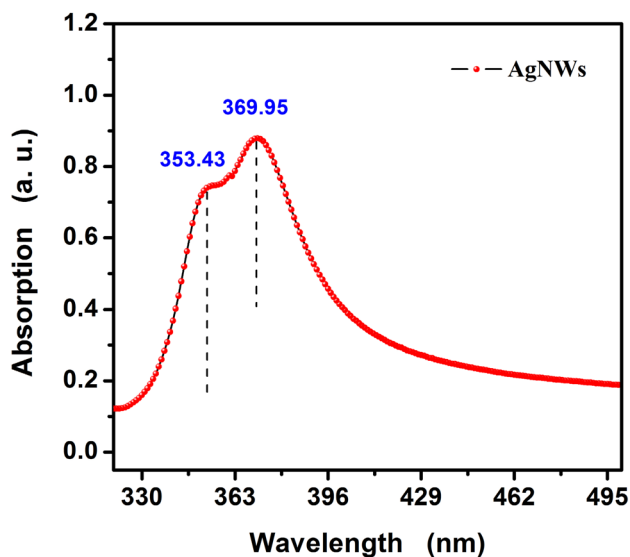

Fig. 6 UV-Vis absorption spectra of the as-prepared AgNWs dispersion

exhibits superior transparency, and a bit hazy is due to light scattering from the AgNWs. Figure 8c shows a typical photograph of an AgNWs mesh on a PET substrate. From the photograph, the AgNWs are uniformly coated on PET substrate, and the film appears to be light blue.

Observe carefully, the AgNW-based TCFs are sufficiently transparent that the logo below the film could be seen clearly. The investigated sheet resistance as a function of a four point probe is summarily shown in Fig. 8d. It can be seen that the sheet resistance of the as-fabricated AgNW-based TCFs can as low as ~ 15 Ω sq^{-1}. In view of the excellent photoelectric properties, the as-fabricated AgNW-based TCFs present more obvious advantages compared with previous reports, including lower haze and sheet resistance, and higher transparency [32–35].

For an efficient TCF, the adhesion is also a very important factor. In order to verify the combination property of the as-fabricated AgNW-based TCFs, an adhesion test was performed by a kapton tape. The results show that the AgNWs mesh possesses strong and excellent adhesion with 0/5B (ISO/ASTM grade) on the PET substrate. Moreover, the AgNW-based TCFs passed 180° reciprocating bend test of 20 times, and have outstanding bending resistance. In practical applications, the stability of AgNW-based TCFs is also one important parameter to determine its reliability and service life. In our incipient experiments, after 60 days exposed to the natural environment, the sheet resistance of AgNW-based TCFs is still near ~ 40 Ω sq^{-1}, which indicates the film surely possess good long-term stability.

Fig. 7 a The photograph of aqueous AgNWs dispersion, and **b** the flexible nature of as-fabricated AgNW-based TCFs
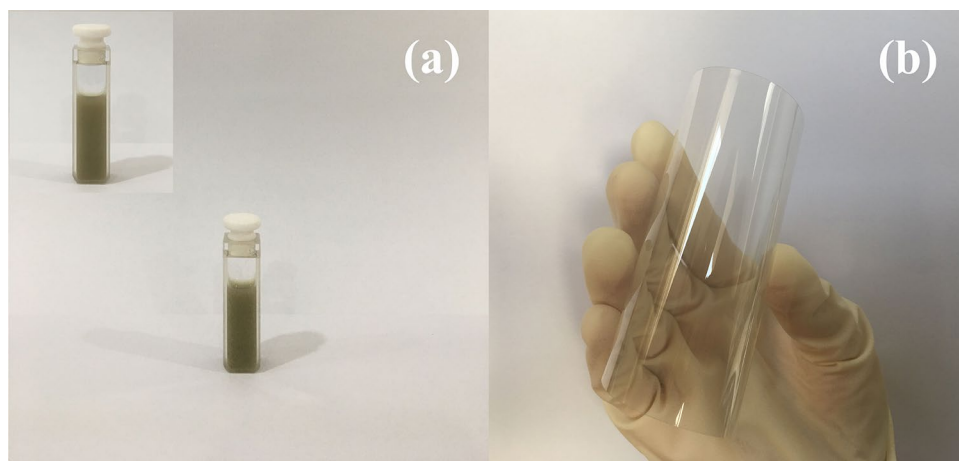
Fig. 8 a, **b** The transmittance and haze based on bare PET substrate and as-fabricated AgNW-based TCFs, **c** the optical photograph of the AgNW-based TCFs, and **d** the sheet resistance of the AgNW-based TCFs
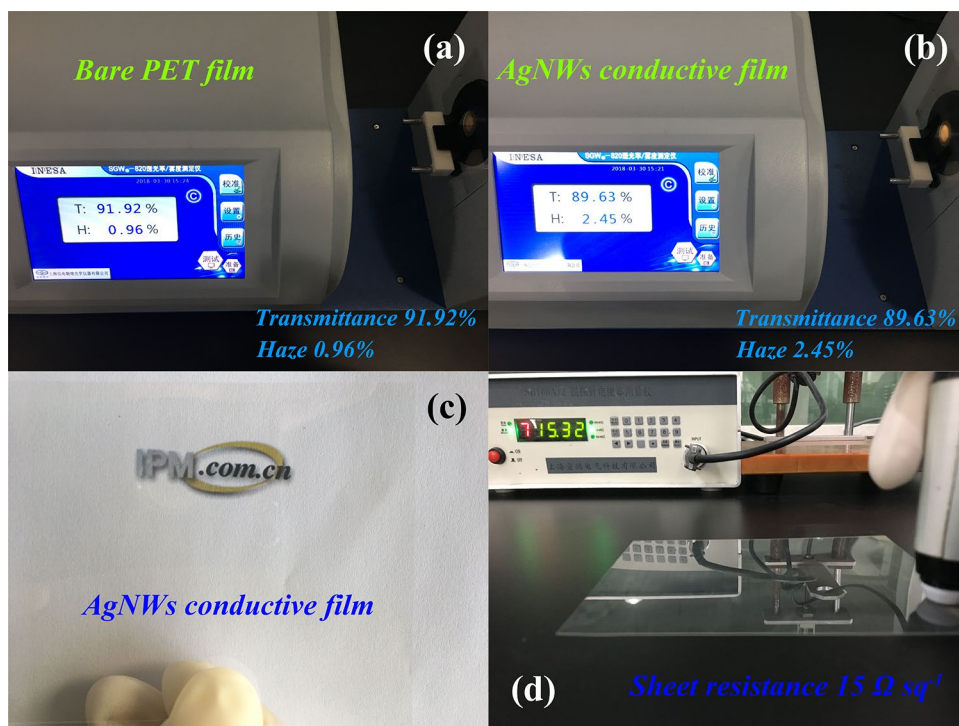
5 Conclusion

In conclusion, we have developed dual ionic assistants assisted synthesis route of ultra-fine AgNWs by solvothermal method without any external pressure. The as-prepared AgNWs exhibits overly thin diameter of ~20 nm and greatly lager aspect ratio of 2000. The flexible TCFs based on as-prepared ultra-fine AgNWs reveal excellent conductivity, low haze, high transparency, and strong adhesion, showing a 97.71% transmittance, a haze of 1.49%, a sheet resistance of ~15 Ω sq^{-1}, and a 0/5B adhesion. The excellent performance suggests that the ultra-fine AgNW-based TCFs can be a promising candidate for using in high-performance optoelectronic devices as a next generation TCF.

References

1. T. Mochizuki, Y. Takigami, T. Kondo, H. Okuzaki, Fabrication of flexible transparent electrodes using PEDOT:PSS and application to resistive touch screen panels. J. Appl. Polym. Sci. **135**, 45972 (2018)

2. S.W. Shin, Y.U. Jung, K.B. Kim, S.W. Choi, S.J. Kang, ITO-free transparent conductive films based on carbon nanomaterials with metal grid for liquid crystal displays. Liq. Cryst. **42**, 1–5 (2015)

3. L.X. Chen, M.H. Lee, Y.W. Wang, Y.S. Lau, A.A. Syed, F.R. Zhu, Interface dipole for remarkable efficiency enhancement in all-solution-processable transparent inverted quantum dot light-emitting diodes. J. Mater. Chem. C **6**, 2596–2603 (2018)

4. J. Liu, F.Z. Luo, A.X. Wei, Z. Liu, Y. Zhao, In-situ growth of Cu_2ZnSnS_4 nanospheres thin film on transparent conducting glass and its application in dye-sensitized solar cells. Mater. Lett. **141**, 228–230 (2015)

5. R. Kumar, R.M. Kumar, D. Lahiri, I. Lahiri, Thermally reduced graphene oxide film on soda lime glass as transparent conducting electrode. Surf. Coat. Tech. **309**, 931–937 (2017)

6. C. Preston, Z.Q. Fang, J. Murray, H.L. Zhu, J.Q. Dai, J.N. Munday, L.B. Hu, Silver nanowire transparent conducting paper-based electrode with high optical haze. J. Mater. Chem. C **2**, 1248–1254 (2014)

7. H.Y. Zhou, Y.L. Wang, J.W. Zhang, Z.K.N. Yu, Y.W. Li, L.C. Tan, Y.W. Chen, A facile approach towards chemical modification of Ag nanowires by PEDOT as a transparent electrode for organic solar cells. J. Mater. Chem. C **6**, 312–319 (2018)

8. J.B. Pyo, B.S. Kim, H. Park, T.A. Kim, C.M. Koo, J. Lee, J.G. Son, S.S. Lee, J.H. Park, Floating compression of Ag nanowire networks for effective strain release of stretchable transparent electrodes. Nanoscale **7**, 16434–16441 (2015)

9. X.L. Chen, X.Z. Wu, S.S. Shao, J.Y. Zhuang, L.M. Xie, S.H. Nie, W.M. Su, Z. Chen, Z. Cui, Hybrid printing metal-mesh transparent conductive films with lower energy photonically sintered copper/tin ink. Sci. Rep. **7**, 13239 (2017)

10. H.G. Im, B.W. An, J. Jin, J. Jang, Y.G. Park, J.U. Park, B.S. Bae, A high-performance, flexible and robust metal nanotrough-embedded transparent conducting film for wearable touch screen panels. Nanoscale **8**, 3916–3922 (2016)

11. J.H. Zhang, Z.F. Chen, X.X. Xu, W. Liao, L.Q. Yang, A simple and efficient approach to fabricate graphene/CNT hybrid transparent conductive films. RSC Adv. **7**, 52555–52560 (2017)

12. P. Chamoli, M.K. Das, K.K. Kar, Urea-assisted low temperature green synthesis of graphene nanosheets for transparent conducting film. J. Phys. Chem. Solids **113**, 17–25 (2018)

13. B.P. Singh, S. Nayak, K.K. Nanda, A. Singh, C. Takai, S. Takashi, M. Fuji, Transparent, flexible, and conducting films based on graphene-polymer composites. Polym. Compos. **39**, 297–304 (2016)

14. S. Devaraju, T. Lee, A.K. Mohanty, Y.K. Hong, K.H. Yoon, Y.S. Lee, J.H. Han, H.J. Paik, Fabrication of durable and flexible single-walled carbon nanotube transparent conductive films. RSC Adv. **7**, 19267–19272 (2017)

15. D. Ito, K. Masuko, B.A. Weintraub, L.C. Mckenzie, J.E. Hutchison, Convenient preparation of ITO nanoparticles inks for transparent conductive thin films. J. Nanopart. Res. **14**, 149–158 (2012)

16. Y.X. Ran, W.W. He, K. Wang, S.L. Ji, C.H. Ye, A one-step route to Ag nanowires with a diameter below 40 nm and an aspect ratio above 1000. Chem. Commun. **50**, 14877–14880 (2014)

17. K. Shahzadi, L. Wu, X.S. Ge, F.H. Zhao, H. Li, S.P. Pang, Y.J. Jiang, J. Guan, X.D. Mu, Preparation and characterization of bio-based hybrid film containing chitosan and silver nanowires. Carbohydr. Polym. **137**, 732–738 (2016)

18. C.Y. Chou, H.S. Liu, G.S. Liou, Highly transparent silver nanowire-polyimide electrode as a snow-cleaning device. RSC Adv. **6**, 61386–61392 (2016)

19. Y. Atwa, N. Maheshwari, I.A. Goldthorpe, Silver nanowire coated threads for electrically conductive textiles. J. Mater. Chem. C **3**, 3908–3912 (2015)

20. S.Y. Chen, Y.W. Guan, Y. Li, X.W. Yan, H.T. Ni, L. Li, A water-based silver nanowire ink for large-scale flexible transparent conductive films and touch screens. J. Mater. Chem. C **5**, 2404–2414 (2017)

21. F. Fang, Y.Q. Li, G.W. Huang, H.M. Xiao, Q.P. Feng, N. Hu, S.Y. Fu, Electrical anisotropy and multidimensional pressure sensor of aligned Fe_3O_4 @ sliver nanowire/polyaniline composite films under an extremely low magnetic field. RSC Adv. **7**, 4260–4268 (2017)

22. S.Q. Liu, B. Weng, Z.R. Tang, Y.J. Xu, Constructing one-dimensional silver nanowire-doped reduced graphene oxide integrated with CdS nanowire network hybrid structures toward artificial photosynthesis. Nanoscale **7**, 861–866 (2015)

23. R. Banica, D. Ursu, T. Nyari, A. Kellenberger, Two step polyol-solvothermal growth of think silver nanowires. Mater. Lett. **194**, 181–184 (2017)

24. Q.T. Tang, H.L. Shen, H.Y. Yao, Y. Jiang, C.F. Zheng, K. Gao, Preparation of silver nanowires/AZO composite film as a transparent conductive material. Ceram. Int. **43**, 1106–1113 (2017)

25. N.D. Zhang, X.S. Yin, H. Gong, Highly conductive and flexible transparent films based on silver nanowire/chitosan composite. RSC Adv. **6**, 47552–47561 (2016)

26. H.W. Du, T. Wan, B. Qu, F.Y. Cao, Q.R. Lin, N. Chen, X. Lin, D.W. Chu, Engineering silver nanowire networks: from transparent electrodes to resistive switching devices. ACS Appl. Mater. Interfaces. **9**, 20762–20770 (2017)

27. L. Zeng, T.S. Zhao, L. An, A high-performance supportless silver nanowire catalyst for anion exchange membrane fuel cells. J. Mater. Chem. A **3**, 1410–1416 (2015)

28. R.R. da Silva, M.X. Yang, S.-I. Choi, M.F. Chi, M. Luo, C. Zhang, Z.Y. Li, P.H.C. Camargo, S.J.L. Ribeiro, Y.N. Xia, Facile synthesis of sub-20 nm silver nanowires through a bromide-mediated Polyol method. ACS Nano **10**, 7892–7900 (2016)

29. B. Li, S.G. Ye, I.E. Stewart, S. Alvarez, B.J. Wiley, Synthesis and purification of silver nanowires to make conducting films with a transmittance of 99%. Nano Lett. **15**, 6722–6726 (2015)

30. W.P. Zhou, A.M. Hu, S. Bai, Y. Ma, D. Bridges, Anisotropic optical properties of large-scale aligned silver nanowire films via controlled coffee ring effects. RSC Adv. **5**, 39103–39109 (2015)

31. E.J. Lee, M.H. Chang, Y.S. Kim, J.Y. Kim, High-pressure polyol synthesis of ultrathin silver nanowires: electrical and optical properties. APL Mater. **1**, 042118 (2013)

32. T.T. Jiu, M. Nogi, T. Sugahara, T. Tokuno, T. Araki, N. Komoda, K. Suganuma, H. Uchida, K. Shinozaki, Strongly adhesive and flexible transparent silver nanowire conductive films fabricated with a high-intensity pulsed light technique. J. Mater. Chem. **22**, 23561–23567 (2012)

33. Y.X. Jin, D.Y. Deng, Y.R. Cheng, L.Q. Kong, F. Xiao, Annealing-free and strongly adhesive silver nanowire networks with long-term reliability by introduction of a nonconductive and biocompatible polymer binder. Nanoscale **6**, 4812–4818 (2014)

34. J.P. Li, S.H. Qi, J. Li, M.Y. Zhang, Z.F. Wang, A highly thermostable and transparent lateral heat spreader based on silver nanowire/polyimide composite. RSC Adv. **5**, 59398–59402 (2015)

35. L. Lian, D. Dong, D.X. Feng, G.F. He, Low roughness silver nanowire flexible transparent electrode by low temperature solution-processing for organic light emitting diodes. Org. Electron. **49**, 9–18 (2017)